Frontiers in Bioscience Landmark

Front. Biosci. (Landmark Ed) **2022**; 27(3): 094
https://doi.org/10.31083/j.fbl2703094

Original Research

Prediction of the Potential Mechanism of Triptolide in Improving Diabetic Nephropathy by Utilizing A Network Pharmacology and Molecular Docking Approach

Xiaofei An[1,†], Decai Fan[2,†], Zi Yin[2], Junhan Zhang[2], Yuexin Zhou[1], Ruina Tian[1], Ming Yan[2,*]

[1]Department of Endocrinology, Affiliated Hospital of Nanjing University of Chinese Medicine, 210004 Nanjing, Jiangsu, China
[2]Institute of Pharmaceutical Science, China Pharmaceutical University, 210009 Nanjing, Jiangsu, China
*Correspondence: brookming@cpu.edu.cn (Ming Yan)
[†]These authors contributed equally.
Academic Editor: Graham Pawelec
Submitted: 23 December 2021 Revised: 21 January 2022 Accepted: 24 February 2022 Published: 9 March 2022

Abstract

Background: Triptolide (TP) is a major active component of colquhounia root tablet, which has been long been used in China to treat diabetic nephropathy (DN) due to its marked anti-inflammatory, antiproteinuric, and podocyte-protective effects. **Methods**: This study investigated the anti-proteinuria activity and related signaling cascade of TP in DN by utilizing a network pharmacology and molecular docking approach. **Results**: From the GeneCard, DisGeNET, and National Center for Biotechnology Information Gene databases, 1458 DN targets were obtained and input together with 303 TP targets into Venny2.1.0 for mapping and comparing. In total, 113 common targets of TP and DN were obtained, of which 7 targets were found to play an important role through theoretical inhibitory constant analysis. The common targets were further analyzed by Kyoto Encyclopedia of Genes and Genomes to identify the pathways related to the therapeutic effect of TP on DN. Among them, the seven targets were found to play key roles in six signaling pathways. The molecular docking results also showed TP had good binding ability to the seven targets. **Conclusions**: Analysis of the common targets and key pathways showed that TP can improve DN via its anti-nephritis, anti-renal fibrosis, antioxidant, and podocyte-protective effects, which might elucidate the mechanism by which TP improves renal function and reduces proteinuria in DN.

Keywords: triptolide; diabetic nephropathy; network pharmacology; molecular docking

1. Introduction

Diabetic nephropathy (DN), a serious microvascular complication of type 1 and type 2 diabetes, is characterized by proteinuria and persistent renal function injury [1]. Proteinuria, an independent risk factor of disease progression, is the most important clinical characteristic of DN, and is also the leading cause of end-stage renal disease [2,3]. Without early intervention, 50% of patients with microalbuminuria will progress to macroalbuminuria [4]. There are many risk factors for the development of DN including increased inflammatory factors and oxidative stress, changes in fat and protein metabolism, and overexpression of the renin-angiotensin-aldosterone system. These lead to the apoptosis and loss of renal podocytes and decreased filtration capacity of glomeruli, thus aggravating DN [5,6]. Although several recent studies have confirmed that angiotensin-converting enzyme inhibitors/angiotensin receptor blockers can reduce DN proteinuria and play a role in delaying disease progression, they are ineffective in DN patients with normal blood pressure [7]. Due to the limitations of traditional Western medical approaches, some DN patients have turned to alternative treatments such as traditional Chinese medicine (TCM).

Triptolide (TP) is a component of the following traditional Chinese herbal medicines: *Tripterygium wilfordii Hook. F.*, *Tripterygium hypoglaucum Levl. Hutch*, *Tripterygium regerii Sprague et Takeda*, and *Tripterygium forretii Dicls* [8]. It is also a major active component of the colquhounia root tablet and tripterygium glycoside tablet, which have long been used in China to treat DN due to their marked anti-inflammatory, anti-proteinuria, and podocyte-protective effects [9–11]. Several randomized controlled clinical trials have indicated that TP possibly imparts nephroprotective effects by decreasing proteinuria, serum creatinine levels, and blood urea nitrogen levels [12–14]. Although TP is effective for improving renal function and reducing proteinuria in DN, the exact mechanism is still unclear.

Network pharmacology is a research method based on virtual computing technology, high-throughput data, and public database, which combines system computing with experiments, introducing a new field of pharmacology [15, 16]. Network pharmacology constructs a multi-level network of disease-phenotype-gene-drug through multi-target interaction [17]. Through analysis of the overall network, we can better predict drug targets to provide help for the re-

Copyright: © 2022 The Author(s). Published by IMR Press.
This is an open access article under the CC BY 4.0 license.

Publisher's Note: IMR Press stays neutral with regard to jurisdictional claims in published maps and institutional affiliations.

search and design of new drugs [18]. For TCM, each component in its prescription has its target, and the effect of the drug is often the result of the synergistic effects of multiple component targets [19]. Network pharmacology can reveal the role of various components at the molecular level so that people can make better use of TCM [20].

In this study, we used network pharmacology to identify the potential targets and signaling pathways of the TCM component TP for the treatment of DN and revealed its possible mechanism. Fig. 1 shows a flowchart of the online pharmacological processes of this study.

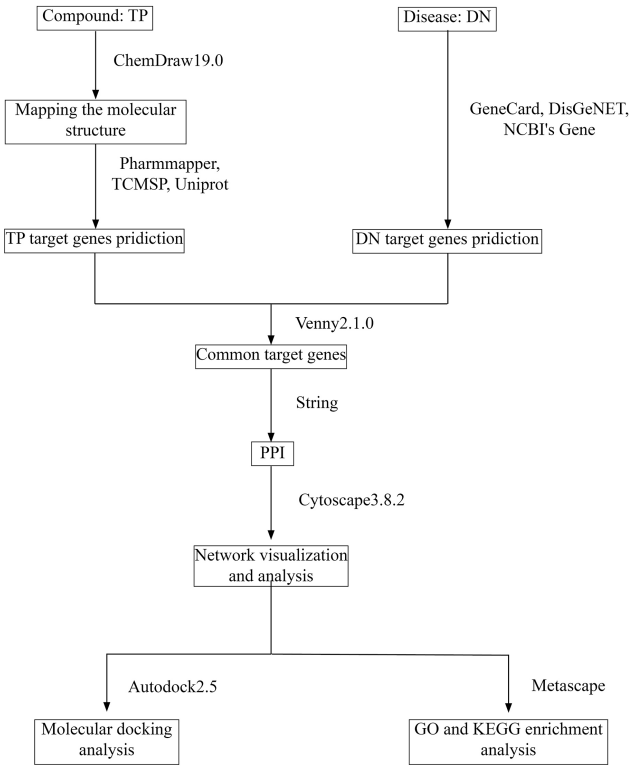

Fig. 1. Network pharmacological workflow to determine the potential mechanisms and targets of triptolide in the treatment of diabetic nephropathy.

2. Methods

2.1 Prediction Targets of TP

The targets of TP were identified by two databases: PharmMapper (http://www.lilab-ecust.cn/pharmmapper/) and traditional Chinese medicine systems pharmacology database and analysis platform (TCMSP) (https://old.tcmsp-e.com/tcmsp.php). The PharmMapper database is a platform for targets prediction, which identifies the potential targets of small molecules by a pharmacophore mapping approach. The chemical structure of TP was drawn by ChemDraw (PerkinElmer, Waltham, MA, USA) and uploaded into the PharmMapper database (Fig. 2). In the PharmMapper database, the maximum number of conformation generation was set to 300 and druggable pharmacophore models were selected as the target set. The names of these target genes were converted to official names by UniProt (https://www.uniprot.org/). TCMSP is a systems pharmacology platform used for screening the active ingredients of TCM. After inputting the keyword "triptolide", targets were obtained from the TCMSP database.

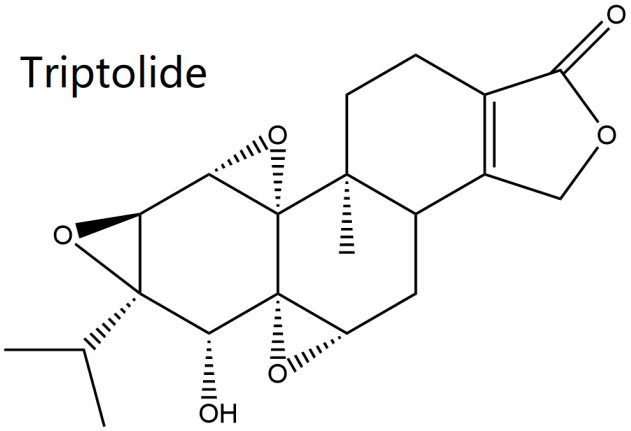

Fig. 2. TP chemical structure.

2.2 Prediction Targets of DN

DN-associated targets were obtained through three online databases, GeneCard (https://www.genecards.org/), DisGeNET (https://www.disgenet.org/), and National Center for Biotechnology Information (NCBI) Gene databases (https://www.ncbi.nlm.nih.gov/gene/). GeneCard is a database with relevant information on proteomics, transcriptomics, and genomics [21]. DisGeNET is a comprehensive database of genes related to human disease [22]. NCBI Gene is a database containing information about multiple species [23]. After searching the keywords "diabetic nephropathy" in the above three databases, the targets of DN were obtained.

2.3 Construction and Analyses of the PPI Network

The potential targets of TP and the disease targets of DN were mapped and compared with the Venny2.1.0 platform (https://bioinfogp.cnb.csic.es/tools/venny/index.html), in order to obtain the common targets of TP and DN. The STRING database (https://string-db.org/) contains almost all known and predicted information about protein-protein interactions, including direct and indirect interactions. The validity of these interactions was calculated in the form of confidence scores, ranging from 0 to 1 [21]. The medium confidence level was set to greater than 0.4, with the species "*Homo sapiens*" [22]. The potential targets of TP and the related targets of TP treatment for DN were uploaded to the STRING database. The protein-protein

IMR Press

interaction networks of TP and TP-DN were obtained [22,23]. Cytoscape (https://cytoscape.org/) is an open source network software platform, which can be used to visualize the intermolecular interaction network and combine network and gene expression profile data [24]. The TP and TP-DN target networks obtained from the STRING database were imported into Cytoscape software (version 3.8.2, Institute for Systems Biology, Seattle, Washington, USA), and the "Network Analyzer" function was used to analyze the topology parameters of the network [25].

2.4 Gene Ontology and Kyoto Encyclopedia of Genes and Genomes Pathway Enrichment Analyses

Metascape database (https://metascape.org/) is a platform for gene annotation analysis, which can analyze the signaling pathways and biological processes of uploaded target genes [26]. For enrichment analysis, the species was set to "*Homo sapiens*", the *p*-value cutoff was 0.05, and other parameters were default [27]. Gene Ontology (GO) annotation and Kyoto Encyclopedia of Genes and Genomes (KEGG) pathway analyses were performed on the targets in turn. The results were saved and sorted according to score, and the relevant biological processes and signal pathways were screened [28]. The results of the filters were put input into a bioinformatics online tool (http://www.bioinformatics.com.cn/), to draw the relevant pictures [29].

2.5 Molecular Docking

The crystal structure of candidate protein binding to TP was obtained from the RCSB Protein Data Bank (https://www.rcsb.org/) and modified using Autodock (version 2.5, Scripps Research, San Diego, California, USA) to remove ligand and water molecules, and add hydrogen and Kollman charge [30,31]. The three-dimensional structure of TP was obtained from DrugBank (https://go.drugbank.com/) and was also modified by Autodock (version 2.5, Scripps Research, San Diego, California, USA) [32]. First, the active site was confirmed by a eutectic small molecule ligand of the proteins. Then the position of the active site with 60 Å outward was taken as the center of the docking box. Second, the Lamarckian genetic algorithm was used to find the best conditions for docking. Finally, the conformation with the lowest energy was selected as the optimal conformation. The docking results were visualized using PyMol (https://pymol.org/2/), where the hydrogen bonds and binding sites were analyzed.

3. Results

3.1 TP-DN Common Targets

A total of 303 targets of TP were obtained through PharmMapper and the TCMSP database. A total of 1458 targets associated with DN were identified in the GeneCard, DisGeNET and NCBI Gene databases. The TP and DN targets were determined using the Venny2.1.0 data platform, which identified common targets (Fig. 3).

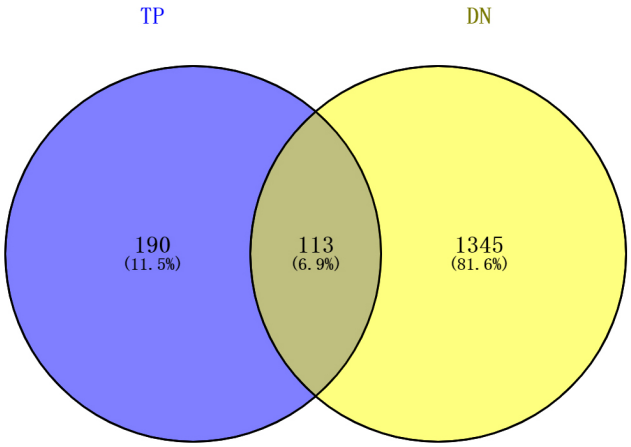

Fig. 3. Venn Diagram of the TP and DN common targets. Note: 303 TP non-common targets (left), 113 TP-DN common targets (middle), 1458 DN non-common targets (right).

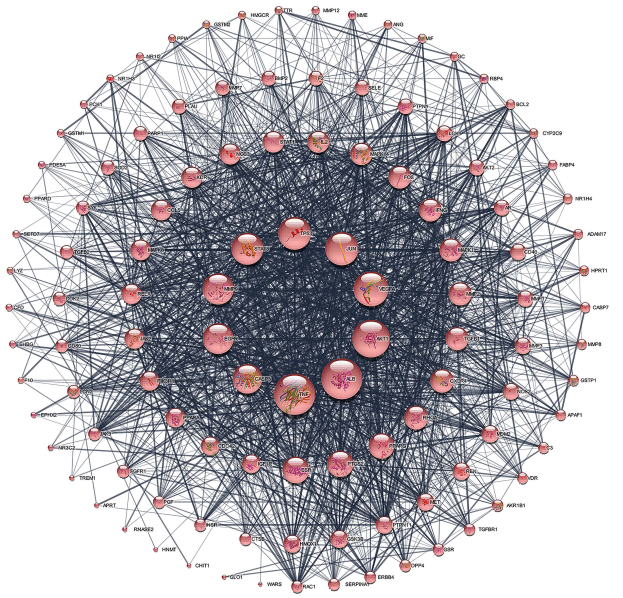

Fig. 4. TP-DN common target network. Note: The nodes size indicates the degree of the target.

3.2 TP-DN Target Network

These common targets were imported into the STRING database, and then the protein-protein interaction relationship was transferred to Cytoscape software to generate the TP-DN target network map (Fig. 4). After analyzing the whole network, 113 nodes and 1618 edges were found, with an average node degree of 28.637 and average local clustering coefficient of 0.648. The nodes in the network were sorted according to the degree value (Table 1), which represent the connection among the nodes in the network (the larger the degree value, the more nodes are associated). Among them, the top 10 targets (tumor necrosis factor [TNF], albumin [ALB], AKT1, vascular endothelial growth factor A [VEGFA], Jun proto-oncogene,

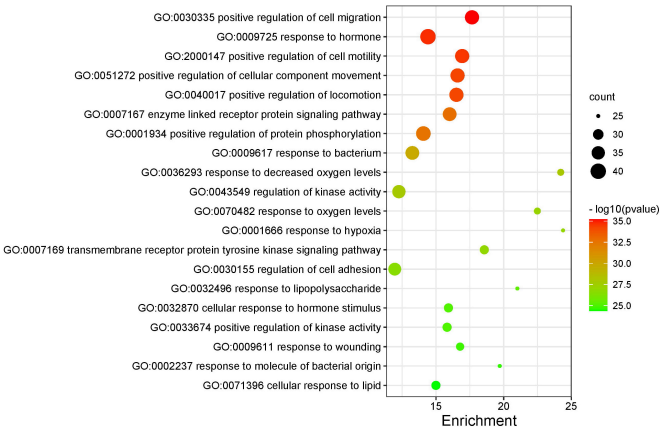

Fig. 5. GO analysis of biological processes. Note: the color scale indicates the adjusted *p*-value, and the dot size represents the gene count in each term.

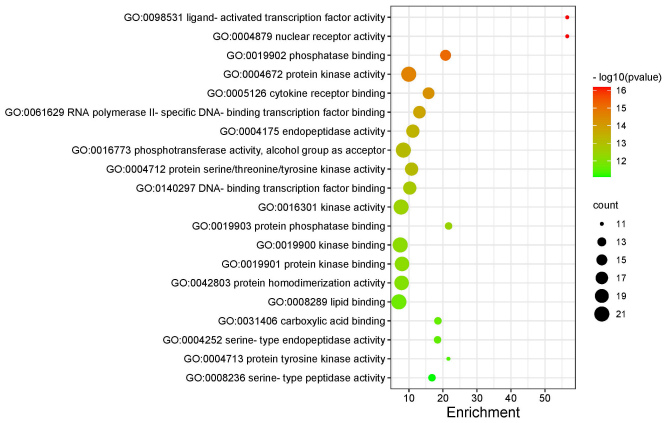

Fig. 7. GO analysis of molecular functions. Note: the color scale indicates the adjusted *p*-value, and the dot size represents the gene count in each term.

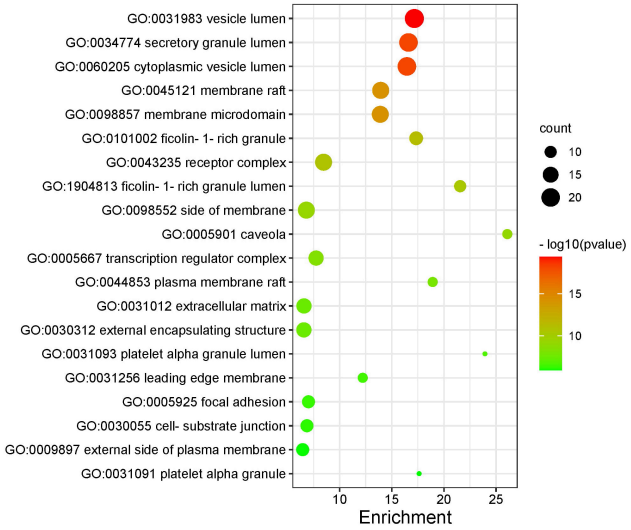

Fig. 6. GO analysis of cell components. Note: the color scale indicates the adjusted *p*-value, and the dot size represents the gene count in each term.

AP-transcription factor subunit [JUN], tumor protein p53 [TP53], signal transducer and activator of transcription 3 (STAT3), matrix metalloproteinase 9 [MMP9], epidermal growth factor receptor [EGFR], caspase 3 [CASP3]) were selected for further molecular docking analysis by degree value.

3.3 Enrichment Analysis of the TP-DN Target Network

The common targets of TP and DN were imported into Metascape for GO and KEGG analyses, and the results were input into a bioinformatics online tool to obtain the enrichment bubble diagram. The results were sorted according to the *p*-value. In GO analysis, the biological processes were found to be associated with the positive regulation of cell migration, response to hormone, positive regulation of cell motility, positive regulation of cell component movement, and positive regulation of locomotion, among others (Fig. 5). The cell components were associated with vesicle lumen, secretory granule lumen, cytoplasmic vesicle lumen, membrane raft, membrane microdomain, among others (Fig. 6). Molecular functions were correlated with ligand activated transcription factor activity, nuclear receptor activity, phosphatase binding, protein kinase activity, and cytokine receptor binding, among others (Fig. 7). In KEGG analysis (Fig. 8), the top pathways related to DN were selected for further analysis and included advanced glycation end product-receptor for advanced glycation end product (AGE-RAGE), mitogen-activated protein kinase (MAPK), phosphoinositide 3-kinase-AKT (PI3K-AKT), relaxin, forkhead box O (FOXO), and TNF signaling pathways.

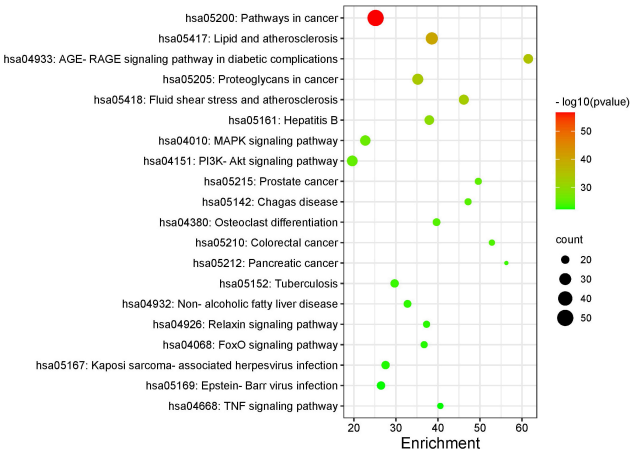

Fig. 8. KEGG pathway analysis. Note: the color scale indicates the adjusted *p*-value, and the dot size represents the gene count in each term.

Table 1. Topological analysis of common target network.

Target name	Abbreviation	ASPL	BC	CC	Clustering coefficient	Degree
Tumor necrosis factor	TNF	1.170	0.124	0.855	0.304	93
Albumin	ALB	1.179	0.106	0.848	0.311	92
AKT Serine/Threonine Kinase 1	AKT1	1.250	0.062	0.800	0.355	84
Vascular endothelial growth factor A	VEGFA	1.313	0.035	0.762	0.415	77
Transcription factor AP-1	JUN	1.348	0.033	0.742	0.434	73
Cellular tumor antigen p53	TP53	1.357	0.031	0.737	0.435	72
Signal transducer and activator of transcription 3	STAT3	1.384	0.022	0.723	0.473	70
Matrix metalloproteinase-9	MMP9	1.402	0.025	0.713	0.448	68
Epidermal growth factor receptor	EGFR	1.411	0.020	0.709	0.463	67
Caspase-3	CASP3	1.429	0.020	0.700	0.485	64
Estrogen receptor alpha	ESR1	1.509	0.020	0.663	0.491	57
Prostaglandin-endoperoxidase synthase 2	PTGS2	1.500	0.015	0.667	0.534	56
Peroxisome proliferator-activated receptor gamma	PPARG	1.527	0.017	0.655	0.497	54
Transforming protein RhoA	RHOA	1.589	0.010	0.629	0.569	50
Chemokine receptor 4	CXCR4	1.598	0.007	0.626	0.595	49
Mitogen-activated protein kinase 1	MAPK1	1.598	0.005	0.626	0.629	48
type IV collagenase	MMP2	1.607	0.006	0.622	0.598	48
Transforming growth factor beta-1	TGFB1	1.589	0.007	0.629	0.603	48
Cellular oncogene fos	FOS	1.598	0.006	0.626	0.603	47
Interferon gamma	IFNG	1.598	0.004	0.626	0.662	47
Mitogen-activated protein kinase 14	MAPK14	1.607	0.005	0.622	0.635	46
Interleukin-2	IL2	1.616	0.005	0.619	0.630	45
Signal transducer and activator of transcription 1	STAT1	1.634	0.022	0.612	0.629	44
Vascular endothelial growth factor receptor 2 variant	KDR	1.634	0.009	0.612	0.591	43
Nitric oxide synthase 3	NOS3	1.652	0.004	0.605	0.657	43
C-C motif chemokine 5	CCL5	1.643	0.004	0.609	0.635	42
Mitogen-activated protein kinase 8	MAPK8	1.643	0.013	0.609	0.551	42
Nuclear Factor Of Kappa Light Polypeptide Gene Enhancer In B-Cells 3	RELA	1.652	0.005	0.605	0.657	41
Janus kinase 2	JAK2	1.661	0.004	0.602	0.670	41
Peroxisome proliferator-activated receptor alpha	PPARA	1.661	0.015	0.602	0.501	39
Phosphatidylinositol 3-kinase regulatory subunit alpha	PIK3R1	1.732	0.004	0.577	0.610	39
Cell division control protein 42 homolog	CDC42	1.696	0.002	0.589	0.722	37
Insulin-like growth factor 1 receptor	IGF1R	1.714	0.004	0.583	0.659	37
Heme oxygenase 1	HMOX1	1.696	0.004	0.589	0.669	35
Glycogen synthase kinase-3 beta	GSK3B	1.705	0.002	0.586	0.708	35
Renin	REN	1.705	0.009	0.586	0.503	34
E3 ubiquitin-protein ligase Mdm2	MDM2	1.732	0.002	0.577	0.709	34
Hepatocyte Growth Factor Receptor	MET	1.732	0.002	0.577	0.727	34
Protein tyrosine phosphatase non-receptor type 11	PTPN11	1.732	0.003	0.577	0.693	34
Matrix metalloproteinase 3	MMP3	1.732	0.007	0.577	0.702	32
Nitric oxide synthase 2	NOS2	1.759	0.002	0.569	0.738	32
Matrix metalloproteinase 1	MMP1	1.768	0.001	0.566	0.772	31
Tumor necrosis factor receptor superfamily member 5	CD40	1.750	0.003	0.571	0.718	31
Tyrosine-protein kinase Lck	LCK	1.768	0.001	0.566	0.777	30
Androgen Receptor	AR	1.768	0.019	0.566	0.655	30
RAC-beta serine/threonine-protein kinase	AKT2	1.768	0.002	0.566	0.715	30
Tyrosine-protein phosphatase non-receptor type 1	PTPN1	1.768	0.002	0.566	0.714	29
E-selectin	SELE	1.786	0.001	0.560	0.775	28
Bone morphogenetic protein 2	BMP2	1.804	0.001	0.554	0.752	27

Table 1. Continued.

Target name	Abbreviation	ASPL	BC	CC	Clustering coefficient	Degree
Prepro-Coagulation Factor II	F2	1.804	0.001	0.554	0.775	27
Matrix metalloproteinase 7	MMP7	1.795	0.006	0.557	0.453	27
Urokinase-type plasminogen activator	PLAU	1.795	0.001	0.557	0.761	27
Protein mono-ADP-ribosyltransferase 1	PARP1	1.786	0.002	0.560	0.683	26
Superoxide dismutase 2	SOD2	1.804	0.002	0.554	0.711	26
Spleen tyrosine kinase	SYK	1.813	0.002	0.552	0.743	25
Cyclin-dependent kinase 2	CDK2	1.830	0.000	0.546	0.848	24
Transforming growth factor beta-2	TGFB2	1.813	0.001	0.552	0.804	24
Neutrophil gelatinase-associated lipocalin	LCN2	1.830	0.002	0.546	0.640	23
CD80 Molecule	CD80	1.821	0.001	0.549	0.775	23
Fibroblast growth factor receptor 1	FGFR1	1.866	0.001	0.536	0.823	22
Janus Kinase 3	JAK3	1.875	0.000	0.533	0.810	22
Cathepsin B	CTSB	1.857	0.001	0.538	0.657	21
Insulin receptor	INSR	1.920	0.002	0.521	0.533	21
Placental growth factor	PGF	1.857	0.002	0.538	0.619	21
Dipeptidyl peptidase 4	DPP4	1.866	0.003	0.536	0.542	20
Glutathione reductase	GSR	1.955	0.000	0.511	0.795	20
Rac Family Small GTPase 1	RAC1	1.839	0.019	0.544	0.516	20
Alpha-1-antitrypsin	SERPINA1	1.946	0.000	0.514	0.789	20
Erb-B2 Receptor Tyrosine Kinase 4	ERBB4	1.848	0.001	0.541	0.721	20
TGF-beta receptor type-1	TGFBR1	1.875	0.000	0.533	0.877	19
Aldo-keto reductase family 1 member B1	AKR1B1	1.848	0.010	0.541	0.725	19
Complement C3	C3	1.875	0.001	0.533	0.752	18
Vitamin D receptor	VDR	1.902	0.002	0.526	0.536	18
Apoptotic protease-activating factor 1	APAF1	1.884	0.001	0.531	0.669	17
Glutathione S-transferase Pi 1	GSTP1	1.893	0.000	0.528	0.853	17
Caspase-7	CASP7	1.902	0.000	0.526	0.775	16
Neutrophil collagenase	MMP8	1.893	0.000	0.528	0.900	16
Disintegrin and metalloproteinase domain-containing protein 17	ADAM17	1.902	0.002	0.526	0.438	15
Hypoxanthine-guanine phosphoribosyltransferase 1	HPRT1	1.902	0.008	0.526	0.695	15
Bile acid receptor	NR1H4	1.911	0.000	0.523	0.771	15
Fatty acid-binding protein 4	FABP4	1.964	0.002	0.509	0.549	14
Apoptosis regulator Bcl-2	BCL2	1.911	0.003	0.523	0.484	14
Cytochrome P450 family 2 subfamily C polypeptide 9	CYP2C9	1.964	0.003	0.509	0.341	14
Retinol-binding protein 4	RBP4	2.009	0.000	0.498	0.725	14
Macrophage migration inhibitory factor	MIF	1.929	0.000	0.519	0.910	13
Group-specific component	GC	1.991	0.002	0.502	0.397	13
Angiogenin	ANG	1.938	0.001	0.516	0.697	12
Atriopeptidase	MME	1.955	0.001	0.511	0.576	12
Hydroxymethylglutaryl-CoA reductase	HMGCR	1.991	0.001	0.502	0.636	11
Macrophage metalloelastase	MMP12	1.955	0.000	0.511	0.836	11
Transthyretin	TTR	1.938	0.001	0.516	0.636	11
Glutathione S-transferase Mu 1	GSTM1	1.946	0.000	0.514	0.756	10
Glutathione S-transferase Mu 2	GSTM2	1.973	0.000	0.507	0.622	10
Oxysterols receptor LXR-alpha	NR1H3	1.946	0.001	0.514	0.578	10
Pregnane X nuclear receptor	NR1I2	1.964	0.000	0.509	0.711	10
Peptidyl-prolyl cis-trans isomerase A	PPIA	1.982	0.001	0.505	0.556	10
Phosphoenolpyruvate carboxykinase 1	PCK1	1.946	0.000	0.514	0.733	10
Peroxisome proliferator-activated receptor delta	PPARD	2.063	0.003	0.485	0.694	9

Table 1. Continued.

Target name	Abbreviation	ASPL	BC	CC	Clustering coefficient	Degree
Histone-lysine N-methyltransferase SETD7	SETD7	1.964	0.000	0.509	0.750	9
cGMP-specific 3',5'-cyclic phosphodiesterase	PDE5A	2.036	0.003	0.491	0.611	9
1,4-beta-N-acetylmuramidase C	LYZ	1.973	0.001	0.507	0.607	8
Complement factor D	CFD	2.009	0.001	0.498	0.607	8
Sex hormone-binding globulin	SHBG	2.018	0.000	0.496	0.821	8
Coagulation factor X	F10	2.054	0.000	0.487	0.800	6
Bifunctional epoxide hydrolase 2	EPHX2	2.089	0.000	0.479	0.600	5
Nuclear receptor subfamily 3 group C member 2	NR3C2	2.411	0.000	0.415	0.400	5
Triggering receptor expressed on myeloid cells 1	TREM1	2.107	0.000	0.475	0.833	4
Adenine phosphoribosyltransferase	APRT	2.134	0.000	0.469	1.000	3
Ribonuclease, RNase A family, 2	RNASE2	2.705	0.000	0.370	0.333	3
Chitotriosidase-1	CHIT1	2.741	0.000	0.365	1.000	2
Histamine N-methyltransferase	HNMT	2.777	0.000	0.360	1.000	2
Lactoylglutathione lyase	GLO1	2.152	0.000	0.465	1.000	2
Tryptophan-tRNA ligase	WARS	2.625	0.000	0.381	0.000	1

Note: ASPL, Average Shortest Path Length; BC, Betweenness Centrality; CC, Closeness Centrality.

3.4 Molecular Docking

The binding ability of TP to the proteins in the TP-DN target network was evaluated by molecular docking. These target proteins included AKT1 (3OCB), ALB (1E7A), CASP3 (1CP3), EGFR (1M17), JUN (1JNM), MMP9 (1GKC), STAT3 (6NJS), TNF (2AZ5), TP53 (6GGA), and VEGFA (4ZFF). Generally, binding energies less than - 5 kcal/mol are considered good binding ability. According to the docking results (Fig. 9), TP had a stronger binding ability with AKT1, EGFR, CASP3, ALB, STAT3, TNF, and TP53. Moreover, TP formed a hydrogen bond with ALA-230 (1.9Å) at the active site of AKT1, TYR-401 (2.1Å), LYS-402 (3.3Å), ASP-549 (2.0Å) of EGFR, GLY-122 (3.5Å), ALA-992 (1.7Å) of CASP3; LYS-721 (1.9Å) and CYS-773 (1.9Å) of ALB; GLN-644 (1.7Å, 2.4Å), GLY-656 (3.4Å), and LYS-658 (1.9Å) of STAT3; GLY-121 (1.9Å) of TNF; and SER-227 (2.2Å) and THR-231 (1.8Å, 2.7Å) of TP53. The detailed binding energies and inhibition constants for the molecular docking of TP are presented in Table 2.

Table 2. The free energies, and theoretical inhibition constants (Ki) of TP binding to targets (at T = 298.15 K).

Class	ΔG (kcal/mol)	Ki (μM)
AKT1	–6.97	7.83
EGFR	–6.85	9.56
CASP3	–6.29	24.49
MMP9	–4.41	584.42
ALB	–6.37	21.58
JUN	–4.98	222.07
STAT3	–7.46	3.4
TNF	–7.27	4.67
TP53	–6.06	36.14
VEGFA	–4.64	399.32

The inhibition constants were obtained from Autodock (version 2.5, Scripps Research, San Diego, California, USA).

4. Discussion

DN is a chronic kidney disease and the leading cause of end-stage renal disease in most developed countries [5]. The causes of DN are complex, but inflammation and oxidative stress are known to be involved in its progression [5,33]. As a new approach, network pharmacology can well analyze the overall relationship between drugs and diseases, including how to participate in the therapeutic process [34]. TP markedly attenuates albuminuria and podocyte injury, regulating the T helper cell balance and macrophage infiltration in an animal model of DN [35,36]. To elucidate the possible mechanism and potential targets of TP in the treatment of DN, we constructed and analyzed the targets through network pharmacology and molecular docking.

Among the 113 TP- and DN-related targets, 7 targets were found to play an essential role through network analysis including ALB, AKT1, CASP3, EGFR, STAT3, TNF, and TP53. Individually, ALB functions as an intravascular transporter, which not only binds a variety of ions, hormones, and drugs but also stabilizes osmotic pressure, anti-inflammation, and antioxidation [37]. When the concentration of glucose is too high, glycosylation of ALB occurs [38]. After additional events, glycosylated ALB further forms AGEs and stimulates cells to produce oxidative stress, thus damaging cells [39]. CASP3 belongs to the family of cysteine proteases and is an essential factor in regulating apoptosis [40]. High glucose can stimulate mito-

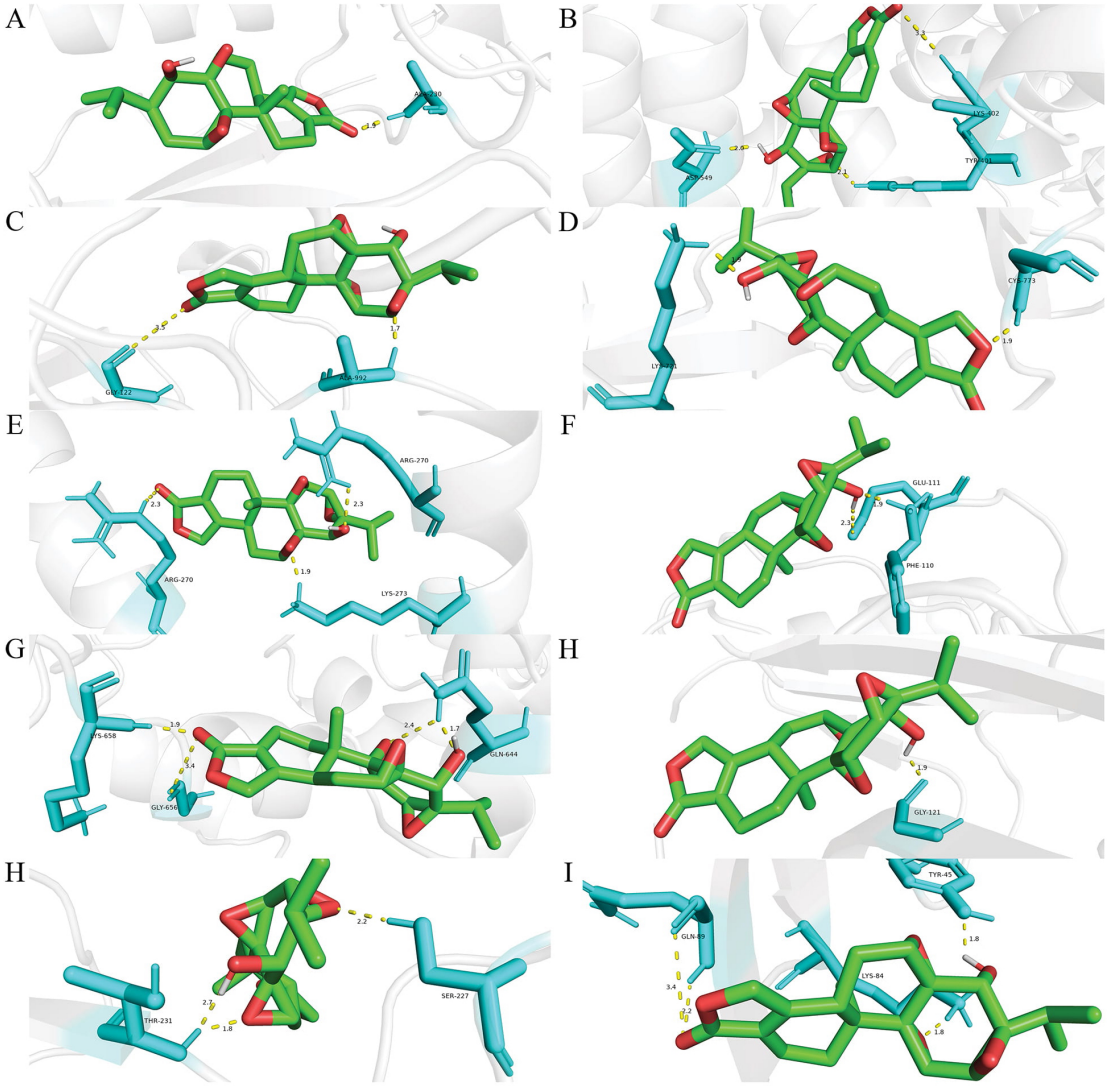

Fig. 9. Molecular docking of TP with potential target proteins A (AKT1), B (ALB), C (CASP3), D (EGFR), E (JUN), F (MMP9), G (STAT3), H (TNF), I (TP53), J (VEGFA). Note: The yellow dotted lines indicate the hydrogen bonds and the numbers above represent their distance. The green structure represents triptolide, and the blue structure indicates the amino acid residues in the binding site of the protein.

chondria, release cytochrome C, and increase the expression of CASP9 and CASP3 [41]. At the same time, activation of CASP12 and CASP3 through endoplasmic reticulum stress can also be independent of mitochondria, resulting in apoptosis [42]. EGFR is an important receptor tyrosine kinase, which is closely related to the development of DN and is widely distributed in glomeruli and renal tubules [43]. EGFR can be activated by high glucose and Src kinase, mediating the phosphorylation of Akt, stimulating a large number of reactive oxygen species (ROS), and inducing the MAPK signal pathway all of which leads to the release of inflammatory factors and reduces insulin secretion in islet cells, resulting in insulin resistance [44]. The Janus kinase/STAT pathway can be activated by high glucose and ROS, and is involved in the pathogenesis of DN [45]. After being phosphorylated, STAT3 enters the nucleus to stimulate the transcription of target genes, increasing the expression of inflammatory and fibrosis factors [46]. Inhibiting the activity of STAT3 can decrease TNF-α and interleukin beta 1 (IL-b1) levels, ameliorating renal fibrosis [47]. In diabetic patients, the levels of inflammatory factors are significantly elevated [48]. As an inflammatory factor, TNF can greatly promote the development of DN and damage the glomerular filtration barrier [49]. Moreover, it can bind to insulin-like growth factor binding protein-3 to induce the apoptosis of mesangial cells [50]. TP53 is a tumor suppressor, which regulates the apoptosis of podocytes [51]. After phosphorylation, AKT1 activates the MAPK signaling pathway, releasing a large number of inflammatory factors and causing renal fibrosis [52].

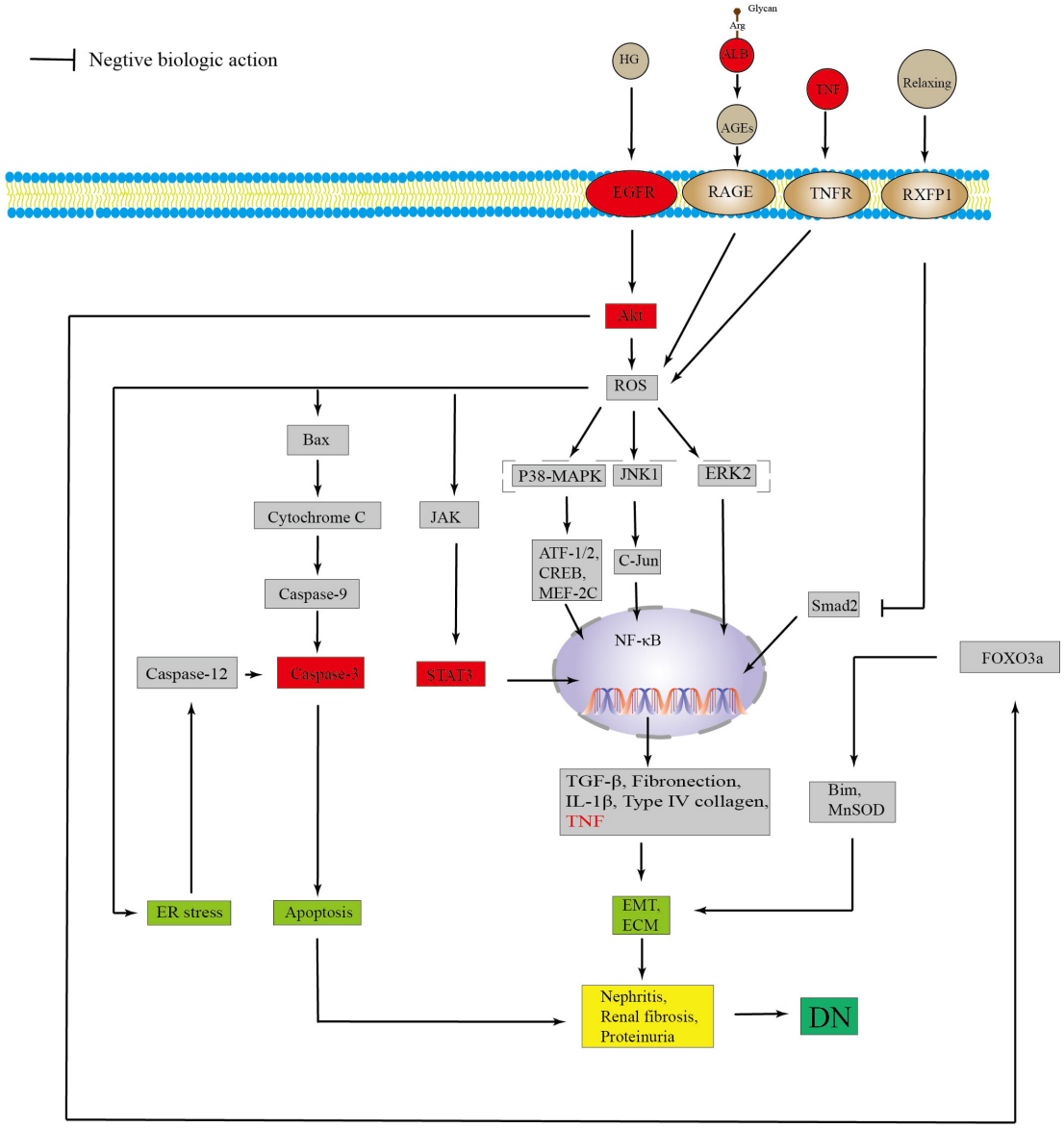

Fig. 10. Schematic diagram of the underlying mechanism of TP in the treatment of DN. High glucose stimulates the EGFR receptor, which activates the PI3K / Akt signaling pathway, which in turn mediates the transcription of genes via the MAPK pathway, leading to TGF-β, Collagen IV, fibronectin as well as TNF-α, IL-1β of the levels rise. The inflammatory factors will trigger ECM and EMT, causing nephritis, renal fibrosis, proteinuria, meanwhile, inflammatory factors will also bind to the corresponding receptors to stimulate cells to release more inflammatory factors. All events ultimately initiate DN.

5. Conclusions

A total of 113 common targets of TP and DN were identified by using network pharmacology, and the binding ability of TP to these targets was verified by molecular docking experiments. After KEGG enrichment analysis, six pathways were found to play a key role in the therapeutic effect of TP on DN (Fig. 10). The MAPK signaling pathway is a classic inflammatory pathway, which is composed of p38-MAPK, c-Jun N-terminal kinase 1 (JNK1), and extracellular signal-regulated kinase 2 (ERK2) [53]. When stimulated by ROS, p38-MAPK, JNK, and ERK release signaling factors such as ATF1/2 and c-Jun that mediate the transcription of transforming growth factor beta (TGF-β), IL-1β, fibronectin, and type IV collagen, leading to nephritis, renal fibrosis, podocyte apoptosis, and proteinuria [54]. A high glucose environment can stimulate the glycosylation of serum ALB and gradually transform it into AGEs [38]. AGEs continuously accumulate and activate RAGE, leading to oxidative stress, activation of the MAPK pathway, chronic inflammation, and eventually renal injury [55–57]. The PI3K/Akt pathway can activate the nuclear factor kappa B (NF-κB) pathway, increasing the expression of IL-6 and leading to glomerular basement membrane thickening and mesangial expansion [52]. Meanwhile, Akt

can phosphorylate FOXO3a in the FOXO signaling pathway, causing extracellular matrix hyperplasia [58]. Relaxin, a member of the insulin family, has vasodilatory and antifibrotic effects. Activation of the relaxin pathway inhibits SMAD2 activation and TGF-β production, reducing synthesis of the extracellular matrix (ECM) [59]. When FOXO3a is phosphorylated by Akt, the expression of bisindolylmaleimide and manganese superoxide dismutase decreases, resulting in ECM accumulation and accelerating the occurrence of DN [60]. Meanwhile, activation of the TNF pathway will elevate the expression of ROS, leading to the altered permeability of the capillary wall and triggering proteinuria [61]. Generally, the results showed that TP could improve DN via its anti-inflammatory, anti-renal fibrosis, anti-oxidant, and podocyte-protective effects.

Data Availability

The data used to support the findings of this study are available from the corresponding author upon request.

Abbreviations

ACEIs, Angiotensin-converting enzyme inhibitors; AGEs, Advanced glycation end products; ALB, Albumin; ASPL, Average shortest path length; ARBs, Angiotensin receptor blockers; BC, Betweenness centrality; CASP3, Caspase-3; CC, Closeness centrality; DN, Diabetic nephropathy; EGFR, Epidermal growth factor receptor; EMT, Epithelial mesenchymal transition; ER, Endoplasmic reticulum; ERK2, Extracellular signal-regulated kinase; ESR1, Estrogen receptor; HG, High glucose; HO-1, Heme oxygenase-1; JAK, Janus kinase; MAPK, Mitogen-activated protein kinase; NF-κB, Nuclear factor kappa B; RAGE, Receptor for advanced glycation end products; ROS, Reactive oxygen species; STAT3, Signal transducer and activator of transcription 3; SRC, SRC proto-oncogene, non-receptor tyrosine kinase; TP53, Tumor protein p53; TGF-β, Transforming growth factor-β; TNF, Tumor necrosis factor; VEGF, Vascular endothelial growth factor.

Author contributions

MY conceived the study, MY and DF designed research; XA, DF, YZ, RT, and JZ performed research; DF, ZY performed data analysis; MY and DF prepared all figures and wrote the manuscript; MY edited the final and prepared the revised manuscript. All authors read and approved the final manuscript.

Ethics approval and consent to participate

Not applicable.

Acknowledgment

We thank Darren Chu from Rutgers University for his linguistic assistance in proofreading this manuscript.

Funding

This work was supported by the National Natural Science Foundation of China (81774248, 82074359), the National Integrative Medicine Key Training Project (2019-44), the Priority Academic Program Development of Jiangsu Higher Education Institutions (PAPD), the Open Projects of the Discipline of Chinese Medicine of the Nanjing University of Chinese Medicine; the Subject of Academic priority discipline of Jiangsu Higher Education Institutions (ZYX03KF027).

Conflict of interest

The authors declare no conflict of interest.

References

[1] Cao Y, Yang Z, Chen Y, Jiang S, Wu Z, Ding B, *et al*. An Overview of the Posttranslational Modifications and Related Molecular Mechanisms in Diabetic Nephropathy. Frontiers in Cell and Developmental Biology. 2021; 9: 630401.

[2] Navarro-González JF, Mora-Fernández C, Muros de Fuentes M, García-Pérez J. Inflammatory molecules and pathways in the pathogenesis of diabetic nephropathy. Nature Reviews. Nephrology. 2011; 7: 327–340.

[3] Zhang J, Zhang Q, Chen X, Liu Y, Xue J, Dahan A, *et al*. Revealing Synergistic Mechanism of Multiple Components in Gandi Capsule for Diabetic Nephropathy Therapeutics by Network Pharmacology. Evidence-Based Complementary and Alternative Medicine. 2018; 2018: 6503126.

[4] Anders H, Huber TB, Isermann B, Schiffer M. CKD in diabetes: diabetic kidney disease versus nondiabetic kidney disease. Nature Reviews. Nephrology. 2019; 14: 361–377.

[5] Koch EAT, Nakhoul R, Nakhoul F, Nakhoul N. Autophagy in diabetic nephropathy: a review. International Urology and Nephrology. 2020; 52: 1705–1712.

[6] A/L B Vasanth Rao VR, Tan SH, Candasamy M, Bhattamisra SK. Diabetic nephropathy: an update on pathogenesis and drug development. Diabetes & Metabolic Syndrome. 2019; 13: 754–762.

[7] Hartman RE, Rao PSS, Churchwell MD, Lewis SJ. Novel therapeutic agents for the treatment of diabetic kidney disease. Expert Opinion on Investigational Drugs. 2020; 29: 1277–1293.

[8] Lv H, Jiang L, Zhu M, Li Y, Luo M, Jiang P, *et al*. The genus Tripterygium: a phytochemistry and pharmacological review. Fitoterapia. 2019; 137: 104190.

[9] Wan F, Tang YW, Tang XL, Li YY, Yang RC. TET2 mediated demethylation is involved in the protective effect of triptolide on podocytes. American Journal of Translational Research. 2021; 13: 1233–1244.

[10] Zhao X, Tang X, Yan Q, Song H, Li Z, Wang D, *et al*. Triptolide ameliorates lupus via the induction of miR-125a-5p mediating Treg upregulation. International Immunopharmacology. 2019; 71: 14–21.

[11] Wang L, Zhang L, Hou Q, Zhu X, Chen Z, Liu Z. Triptolide attenuates proteinuria and podocyte apoptosis via inhibition of NF-kappaB/GADD45B. Scientific Reports. 2018; 8: 10843.

[12] Wang D, Zhao X, Cui Y, Zhang T, Wang F, Hu Y. Efficacy and safety of Tripterygium wilfordii Hook F for CKD in Mainland China: a systematic review and meta-analysis. Phytotherapy Research: PTR. 2018; 32: 436–451.

[13] Xiong C, Li L, Bo W, Chen H, XiaoWei L, Hongbao L, *et al*. Evaluation of the efficacy and safety of TWHF in diabetic nephropathy patients with overt proteinuria and normal eGFR.

Journal of the Formosan Medical Association. 2020; 119: 685–692.
[14] Lengnan X, Ban Z, Haitao W, Lili L, Aiqun C, Huan W, *et al*. Tripterygium wilfordii Hook F Treatment for Stage IV Diabetic Nephropathy: Protocol for a Prospective, Randomized Controlled Trial. BioMed Research International. 2020; 2020: 981037.
[15] Mou X, Zhou DY, Zhou D, Liu K, Chen LJ, Liu WH. A bioinformatics and network pharmacology approach to the mechanisms of action of Shenxiao decoction for the treatment of diabetic nephropathy. Phytomedicine. 2020; 69: 153192.
[16] Song X, Zhang Y, Dai E, Du H, Wang L. Mechanism of action of celastrol against rheumatoid arthritis: a network pharmacology analysis. International Immunopharmacology. 2019; 74: 105725.
[17] Liu Z, Sun X. [Network pharmacology: new opportunity for the modernization of traditional Chinese medicine] Yao Xue Xue Bao. 2012; 47: 696–703.
[18] Fang T, Liu L, Liu W. Network pharmacology-based strategy for predicting therapy targets of Tripterygium wilfordii on acute myeloid leukemia. Medicine. 2020; 99: e23546.
[19] Yuan H, Ma Q, Cui H, Liu G, Zhao X, Li W, *et al*. How can Synergism of Traditional Medicines Benefit from Network Pharmacology? Molecules. 2017; 7.
[20] Zhang R, Yu S, Bai H, Ning K. TCM-Mesh: the database and analytical system for network pharmacology analysis for TCM preparations. Scientific Reports. 2018; 7: 2821.
[21] Szklarczyk D, Gable AL, Lyon D, Junge A, Wyder S, Huerta-Cepas J, *et al*. STRING v11: protein–protein association networks with increased coverage, supporting functional discovery in genome-wide experimental datasets. Nucleic Acids Research. 2019; 47: D607–D613.
[22] Guo X, Ji J, Feng Z, Hou X, Luo Y, Mei Z. A network pharmacology approach to explore the potential targets underlying the effect of sinomenine on rheumatoid arthritis. International Immunopharmacology. 2020; 80: 106201.
[23] Guo M, Dai Y, Gao J, Chen P. Uncovering the Mechanism of Astragalus membranaceus in the Treatment of Diabetic Nephropathy Based on Network Pharmacology. Journal of Diabetes Research. 2020; 2020: 5947304.
[24] Shannon P, Markiel A, Ozier O, Baliga NS, Wang JT, Ramage D, *et al*. Cytoscape: a software environment for integrated models of biomolecular interaction networks. Genome Research. 2004; 13: 2498–2504.
[25] Assenov Y, Ramírez F, Schelhorn S, Lengauer T, Albrecht M. Computing topological parameters of biological networks. Bioinformatics. 2008; 24: 282–284.
[26] Zhou Y, Zhou B, Pache L, Chang M, Khodabakhshi AH, Tanaseichuk O, *et al*. Metascape provides a biologist-oriented resource for the analysis of systems-level datasets. Nature Communications. 2019; 10: 1523.
[27] Chai S, Huang X, Wu T, Xu S, Ren W, Yang G. Comparative genomics reveals molecular mechanisms underlying health and reproduction in cryptorchid mammals. BMC Genomics. 2021; 22: 763.
[28] Yu J, Yuan H, Bao L, Si L. Interaction between piperine and genes associated with sciatica and its mechanism based on molecular docking technology and network pharmacology. Molecular Diversity. 2021; 25: 233–248.
[29] Bardou P, Mariette J, Escudié F, Djemiel C, Klopp C. Jvenn: an interactive Venn diagram viewer. BMC Bioinformatics. 2014; 15: 293.
[30] Berman HM, Westbrook J, Feng Z, *et al*. The Protein Data Bank. Nucleic Acids Research 2000; 28: 235–242.
[31] Sanner MF. Python: a programming language for software integration and development. Journal of Molecular Graphics & Modelling. 1999; 17: 57–61.
[32] Wishart DS, Feunang YD, Guo AC, Lo EJ, Marcu A, Grant JR, *et al*. DrugBank 5.0: a major update to the DrugBank database for 2018. Nucleic Acids Research. 2018; 46: D1074–D1082.
[33] Bhattacharjee N, Barma S, Konwar N, Dewanjee S, Manna P. Mechanistic insight of diabetic nephropathy and its pharmacotherapeutic targets: an update. European Journal of Pharmacology. 2016; 791: 8–24.
[34] Ye H, Wei J, Tang K, Feuers R, Hong H. Drug Repositioning through Network Pharmacology. Current Topics in Medicinal Chemistry. 2016; 16: 3646–3656.
[35] Ma R, Liu L, Liu X, Wang Y, Jiang W, Xu L. Triptolide markedly attenuates albuminuria and podocyte injury in an animal model of diabetic nephropathy. Experimental and Therapeutic Medicine. 2019; 6: 649–656.
[36] Guo H, Pan C, Chang B, Wu X, Guo J, Zhou Y, *et al*. Triptolide Improves Diabetic Nephropathy by Regulating Th Cell Balance and Macrophage Infiltration in Rat Models of Diabetic Nephropathy. Experimental and Clinical Endocrinology & Diabetes. 2016; 124: 389–398.
[37] Li Z, Liu J, Wang W, Zhao Y, Yang D, Geng X. Investigation of hub genes involved in diabetic nephropathy using biological informatics methods. Annals of Translational Medicine. 2020; 8: 1087.
[38] Zendjabil M. Glycated albumin. Clinica Chimica Acta. 2020; 502: 240–244.
[39] Vetter SW. Glycated Serum Albumin and AGE Receptors. Advances in Clinical Chemistry. 2015; 72: 205–275.
[40] Choudhary GS, Al-Harbi S, Almasan A. Caspase-3 activation is a critical determinant of genotoxic stress-induced apoptosis. Methods in Molecular Biology. 2015; 1219: 1–9.
[41] Mishra R, Emancipator SN, Kern T, Simonson MS. High glucose evokes an intrinsic proapoptotic signaling pathway in mesangial cells. Kidney International. 2005; 67: 82–93.
[42] Brezniceanu M, Lau CJ, Godin N, Chénier I, Duclos A, Éthier J, *et al*. Reactive Oxygen Species Promote Caspase-12 Expression and Tubular Apoptosis in Diabetic Nephropathy. Journal of the American Society of Nephrology. 2010; 21: 943–954.
[43] Panchapakesan U, Pollock C, Saad S. Renal epidermal growth factor receptor: its role in sodium and water homeostasis in diabetic nephropathy. Clinical and Experimental Pharmacology & Physiology. 2011; 38: 84–88.
[44] Xu Z, Zhao Y, Zhong P, Wang J, Weng Q, Qian Y, *et al*. EGFR inhibition attenuates diabetic nephropathy through decreasing ROS and endoplasmic reticulum stress. Oncotarget. 2017; 8: 32655–32667.
[45] Chuang PY, He JC. JAK/STAT signaling in renal diseases. Kidney International. 2010; 78: 231–234.
[46] Said E, Zaitone SA, Eldosoky M, Elsherbiny NM. Nifuroxazide, a STAT3 inhibitor, mitigates inflammatory burden and protects against diabetes-induced nephropathy in rats. Chemico-Biological Interactions. 2018; 281: 111–120.
[47] Zheng C, Huang L, Luo W, Yu W, Hu X, Guan X, *et al*. Inhibition of STAT3 in tubular epithelial cells prevents kidney fibrosis and nephropathy in STZ-induced diabetic mice. Cell Death & Disease. 2019; 10: 848.
[48] Chen Y, Qiao Y, Xu Y, Ling W, Pan Y, Huang Y, *et al*. Serum TNF-α concentrations in type 2 diabetes mellitus patients and diabetic nephropathy patients: a systematic review and meta-analysis. Immunology Letters. 2017; 186: 52–58.
[49] Navarro JF, Mora-Fernández C. The role of TNF-alpha in diabetic nephropathy: pathogenic and therapeutic implications. Cytokine & Growth Factor Reviews. 2006; 17: 441–450.
[50] Vasylyeva TL, Chen X, Ferry RJ. Insulin-like growth factor binding protein-3 mediates cytokine-induced mesangial cell apoptosis. Growth Hormone & IGF Research. 2005; 15: 207–

214.
[51] Zhang SZ, Qiu XJ, Dong SS, *et al*. MicroRNA-770-5p is involved in the development of diabetic nephropathy through regulating podocyte apoptosis by targeting TP53 regulated inhibitor of apoptosis 1. European Review for Medical and Pharmacological Sciences. 2019; 23: 1248–1256.
[52] Wang X, Yao M, Liu S, Hao J, Liu Q, Gao F. Interplay between the Notch and PI3K/Akt pathways in high glucose-induced podocyte apoptosis. American Journal of Physiology-Renal Physiology. 2014; 306: F205–F213.
[53] Sun Y, Liu W, Liu T, Feng X, Yang N, Zhou H. Signaling pathway of MAPK/ERK in cell proliferation, differentiation, migration, senescence and apoptosis. Journal of Receptor and Signal Transduction Research. 2015; 35: 600–604.
[54] Qiu Y, Tang L. Roles of the NLRP3 inflammasome in the pathogenesis of diabetic nephropathy. Pharmacological Research. 2016; 114: 251–264.
[55] Jha JC, Banal C, Chow BSM, Cooper ME, Jandeleit-Dahm K. Diabetes and Kidney Disease: Role of Oxidative Stress. Antioxidants & Redox Signaling. 2016; 25: 657–684.
[56] Wang Z, Zhang J, Chen L, Li J, Zhang H, Guo X. Glycine Suppresses AGE/RAGE Signaling Pathway and Subsequent Oxidative Stress by Restoring Glo1 Function in the Aorta of Diabetic Rats and in HUVECs. Oxidative Medicine and Cellular Longevity. 2019; 2019: 4628962.
[57] Sanajou D, Ghorbani Haghjo A, Argani H, Aslani S. AGE-RAGE axis blockade in diabetic nephropathy: Current status and future directions. European Journal of Pharmacology. 2018; 833: 158–164.
[58] Xue M, Cheng Y, Han F, Chang Y, Yang Y, Li X, *et al*. Triptolide Attenuates Renal Tubular Epithelial-mesenchymal Transition via the MiR-188-5p-mediated PI3K/AKT Pathway in Diabetic Kidney Disease. International Journal of Biological Sciences. 2018; 14: 1545–1557.
[59] Xie X, Xia W, Fei X, Xu Q, Yang X, Qiu D, *et al*. Relaxin Inhibits High Glucose-Induced Matrix Accumulation in Human Mesangial Cells by Interfering with TGF-β1 Production and Mesangial Cells Phenotypic Transition. Biological & Pharmaceutical Bulletin. 2015; 38: 1464–1469.
[60] Kato M, Yuan H, Xu Z, Lanting L, Li S, Wang M, *et al*. Role of the Akt/FoxO3a pathway in TGF-beta1-mediated mesangial cell dysfunction: a novel mechanism related to diabetic kidney disease. Journal of the American Society of Nephrology. 2006; 17: 3325–3335.
[61] Abouzed TK, Sadek KM, Ghazy EW, Abdo W, Kassab MA, Hago S, *et al*. Black mulberry fruit extract alleviates streptozotocin-induced diabetic nephropathy in rats: targeting TNF-α inflammatory pathway. Journal of Pharmacy and Pharmacology. 2020; 72: 1615–1628.